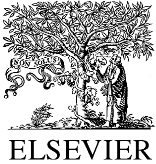
ELSEVIER

Available online at www.sciencedirect.com
SCIENCE DIRECT®

Microelectronic Engineering 67–68 (2003) 56–62

MICROELECTRONIC ENGINEERING

www.elsevier.com/locate/mee

Sub-50 nm period patterns with EUV interference lithography

H.H. Solak[a,*], C. David[a], J. Gobrecht[a], V. Golovkina[b], F. Cerrina[b], S.O. Kim[b], P.F. Nealey[b]

[a]*Laboratory for Micro and Nanotechnology, Paul Scherrer Institute, Villigen CH-5232, Switzerland*
[b]*Center for Nanotechnology, University of Wisconsin-Madison, Madison, WI 53706, USA*

Abstract

We have used transmission diffraction gratings in an interferometric setup to pattern one- and two-dimensional periodic patterns with periods near 50 nm. The diffraction gratings were written with e-beam lithography. The exposures were made at 13.4 nm wavelength with undulator radiation, which provides spatially coherent radiation. This technique offered a multiplication of pattern frequency by a factor of 2 and $\sqrt{2}$ in the one- and two-dimensional cases, respectively. Interference lithography with gratings offers a number of advantages, including achromaticity and insensitivity to misalignment. The demonstrated structures include line/space patterns with 45 nm period and a square array of holes with 56 nm period.
© 2003 Elsevier Science B.V. All rights reserved.

Keywords: Interference lithography; Multiple beam; Extreme ultraviolet; Diffraction grating; Undulator

1. Introduction

Interference lithography (IL) is commonly used for making periodic patterns for research and production uses. It provides a way to achieve or approach the ultimate resolution for a certain wavelength without requiring complicated and expensive high numerical aperture optics. Advantages of IL technique include practically unlimited depth of focus and large exposure fields.

Lasers are used as sources in IL in visible and ultraviolet regions thanks to their excellent coherence properties. The smallest period reachable with IL is equal to half of the wavelength. Therefore for periods smaller than ~75 nm, lasers have to be replaced by other sources that have smaller wavelengths. Extreme ultraviolet (EUV) light from undulators at synchrotron radiation facilities has long been recognized as a possible source for IL in this regime [1]. An interferometer based on reflective optics using EUV light has recently been demonstrated to produce 38 nm period gratings

*Corresponding author.
E-mail address: harun.solak@psi.ch (H.H. Solak).

0167-9317/03/$ – see front matter © 2003 Elsevier Science B.V. All rights reserved.
doi:10.1016/S0167-9317(03)00059-5

[2]. However, the technique requires temporally coherent light, which limits the number of periods produced. This limits the usefulness of undulator radiation with this type of interferometer, since undulator radiation has a relatively large spectral width, typically in the order of a few percents.

This difficulty is overcome by the use of achromatic interferometers that are based on transmission diffraction gratings. An earlier demonstration of this type attempted with an undulator source produced 50 nm period gratings, albeit with poor quality attributed to effects of vibrations in the system [3]. More recently a multiple beam scheme using diffraction gratings was introduced, with which 140 nm period hole arrays were demonstrated [4]. This approach depends on gratings fabricated with e-beam lithography. The interference system achieves a multiplication of grating spatial frequency with the multiplication factor depending on the beam geometry. In this report we describe recent advances we made in this area, which allowed us to produce high quality structures in photoresist with periods below 50 nm.

2. Experiment

The materials for making EUV transmission gratings are selected based on their absorption and phase shifting properties as well as fabrication process related considerations. The high absorption of all materials at this wavelength region requires use of extremely thin support membranes. Fig. 1 shows a schematic cross-section of diffracting structures on a 100 nm-thick Si_3N_4 membrane. The fabrication process starts with the deposition of a thin film of Cr on the membrane. Then the sample is coated with a 40 nm-thick PMMA layer and grating patterns are exposed with low voltage e-beam lithography at 2.5 keV. After the development in 1:3 MIBK:IPA solution for 30 s, the structures are exposed with the electron beam machine again to cross-link the PMMA. This increases the resistance of PMMA to the subsequent dry etching of the underlying Cr layer. Fig. 2 demonstrates the beneficial effect of this step, showing the much higher quality of transferred patterns in the area where the PMMA structures were exposed after the development. In principle the Cr structures can be used as a diffraction grating, but in order to increase the efficiency, we etched ~40 nm into the Si_3N_4 membrane using the Cr as a hard etch mask, again using reactive ion etching. Calculated efficiency for this structure is plotted in Fig. 3 as a function of the Cr layer thickness and etch depth into the Si_3N_4. Here the diffraction efficiency is defined as the ratio of the first order diffracted light intensity exiting the membrane to the intensity of the incident light on the grating. Therefore the calculation results include the absorption by the remaining support membrane. The silicon nitride membrane total thickness is taken as a constant 100 nm. The improvement in efficiency with higher nitride etch depth is due to the combined effects of favorable phase shift in the resulting grating bars and the removal of the Si_3N_4 in the area between the grating bars, which would otherwise absorb and attenuate the transmitted light. In our typical process of 25 nm Cr film thickness and 40 nm Si_3N_4 etch depth, we expect to have reached 6% efficiency. Etching deeper into the Si_3N_4 layer would improve the

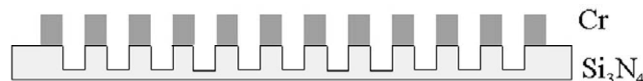

Fig. 1. Schematic cross-section of a diffraction grating. Typically the Cr layer was 25 nm-thick and the etch depth into Si_3N_4 membrane was 40 nm.

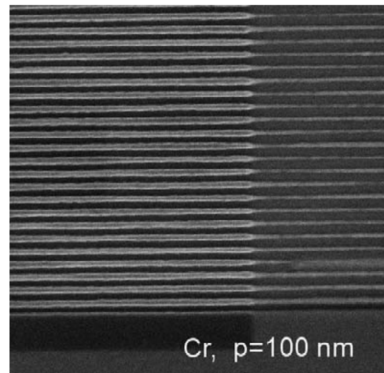

Fig. 2. SEM image of a 100 nm period grating after the Cr etching step. The area on the right hand side with wider and better defined Cr lines was exposed with 2.5-keV electrons after the PMMA development step to cross-link the resist here, thus increasing its etch resistance.

efficiency but the membranes become weaker and more fragile as the remaining thickness is reduced. In practice most failures occur during the etching of the Si_3N_4 layer where the thermal load may be responsible for increased stress and eventual rupture of the membrane. For membranes surviving this RIE step, later spontaneous breakage is very rare. Fig. 4 shows 70 and 100 nm period gratings after Cr and Si_3N_4 etching steps, respectively.

The EUV exposures were performed at the EUV station of the Center for Nanotechnology at the Synchrotron Radiation Center [5]. The beamline has an option to bring wide band undulator light into the exposure chamber after three bounces from multilayer-coated flat mirrors. The calculated spectral width, $\Delta\lambda/\lambda$, is 2% for this beam. The other option is to bring light through a spherical grating

Fig. 3. Calculated diffraction efficiency for the structure shown in Fig. 1 as a function of the Cr film thickness and the Si_3N_4 etch depth. The Si_3N_4 membrane thickness was taken as 100 nm.

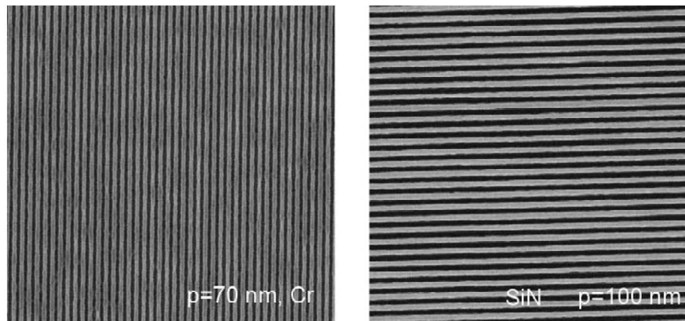

Fig. 4. (a,b) SEM images of 70 and 100 nm period e-beam written gratings after Cr and Si_3N_4 etch steps, respectively.

monochromator, which reduces the bandwidth down to 0.1% at the expense of reduced flux. Since the present interference scheme is achromatic, we chose the former option to take advantage of the higher flux. The quality of the achieved results indicate high modulation in the interference pattern confirming the achromaticity of the scheme.

The source to sample distance of 14 m and the source size of 800 μm and 80 μm in horizontal and vertical directions should provide lateral coherence of approximately 250 μm and 2.5 mm in these directions, respectively. However imperfections of the flat multilayer mirror surfaces in the form of low spatial frequency undulations (figure error) and roughness can greatly reduce this length. In addition vibrations of the sample assembly with respect to the source may broaden the source size seen by the sample during the exposure time, which effectively reduces the transverse coherence length. The required coherence length is determined by the size of the desired exposure area. For our exposure area of 50×50 μm^2 in this experiment, the required coherence length was ~100 μm. Our results indicate that the system provided light with coherence length better than 100 μm, including effects such as vibrations and beam instabilities.

Fig. 5(a) shows the geometry for making one-dimensional gratings (line/space) patterns. The ±1st order diffracted beams from the two grating interfere in the center to form a fringe pattern which has

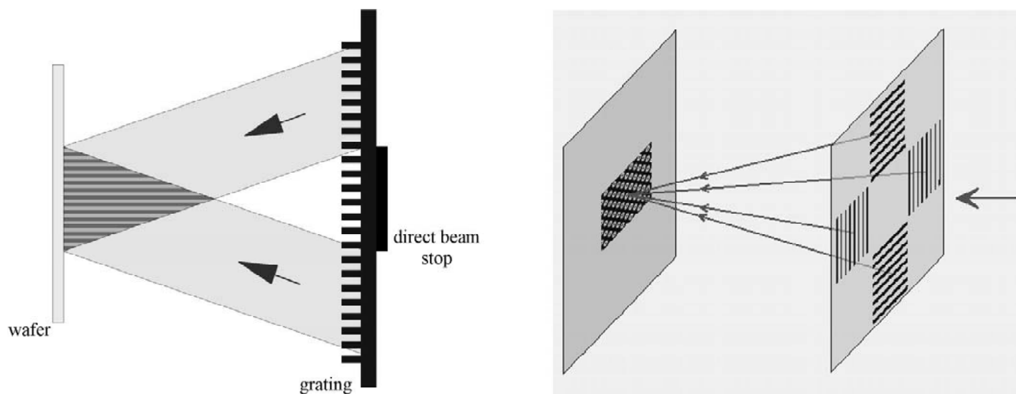

Fig. 5. Schemes for (a) two-beam interference and (b) four-beam interference.

double the frequency of the diffraction gratings. The patterned area has the same width as the diffraction gratings, which was 50 μm in this experiment. The scheme for two-dimensional gratings is shown in Fig. 5(b) where four square shaped gratings diffract into a central area which has the same shape and size as the diffraction gratings. The phases of the four gratings were written in the e-beam lithography machine so as to obtain in − phase addition of all the beams, on a 45° rotated square grid [6,7]. The frequency of the intensity pattern is $\sqrt{2}$ times the frequency of the diffraction gratings.

In both the one- and two-dimensional geometries intensity oscillations due to Fresnel diffraction were observed near the edges of the patterned area. A straightforward analysis indicates that the relative area of this non-uniformity is inversely proportional to the number of periods in the gratings. In practical applications of this technique the gratings should be designed to be larger than the desired pattern area so that the affected edge areas can be excluded later.

The EUV exposures were done on Si wafers coated with 40 nm-thick PMMA films. After exposure the samples were developed in 1:3 solution of MIBK:IPA for 30 s. Typical exposure times varied in the 30–60-s range depending on the electron beam current in the storage ring.

3. Results

The two SEM images in Fig. 6 show EUV exposed gratings with 45 and 52.5 nm periods. The e-beam written diffraction gratings used to create these had 90 and 105 nm periods, respectively. Given the 40 nm PMMA thickness and 22.5 and 26.25 nm half pitch of the line/space patterns, the height-to-width aspect ratios of these lines were close to 2. Despite their small linewidth and moderately high aspect ratio the PMMA structures were to a large degree collapse free. This observation points to an advantage of EUV exposures over e-beam where forward scattering of electrons results in deposition of a higher dose near the resist substrate interface. This dose distribution causes some degree of undercut in the developed resist profile making the structures more vulnerable to collapse problems during the development step. On the other hand the dose distribution

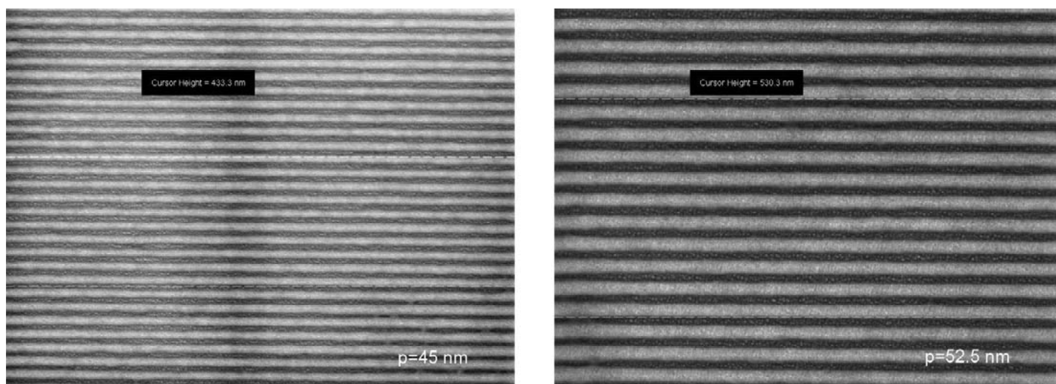

Fig. 6. Line/space patterns exposed in PMMA with EUV interference lithography with periods of (a) 45 nm and (b) 52.5 nm.

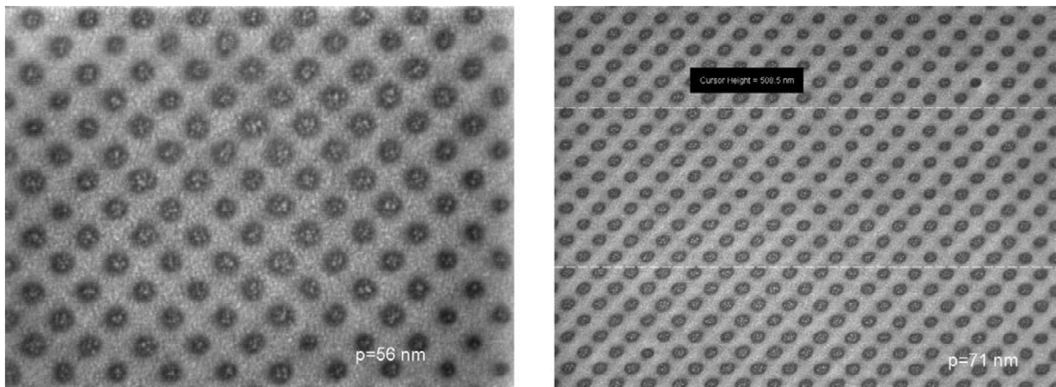

Fig. 7. Two-dimensional arrays of holes in PMMA exposed with EUV interference lithography with periods of (a) 56 nm and (b) 71 nm. A thin Au film was sputter deposited on the sample to avoid charging during the SEM examination.

in EUV decreases slightly towards the resist bottom. Therefore the EUV exposed positive resist structures become stronger toward the base making them stand better against forces inducing collapse.

Examples of two-dimensional patterns created with EUV IL are shown in Fig. 7, where 80 and 100 nm period diffraction gratings were used to make the 56 and 71 nm period hole arrays, respectively. Array of posts can be made either by using a negative resist or changing the phase relation of the four gratings in the e-beam created mask [6,7]. An added advantage of the latter method is that the frequency multiplication factor is 2 instead of $\sqrt{2}$ achieved in the presented results. The hole sizes in these images seem to show some variation with no apparent long or short range order, in a seemingly random manner. This behavior may have origins similar to line edge roughness in line/space patterns, such as statistical nature of the development process or shot noise effects in exposure. This interesting point requires further experimentation and analysis which may shed light onto the origins of line edge roughness in advanced lithographic processes in general.

4. Conclusions

The present results demonstrate the fabrication of high-resolution gratings with EUV IL. This technique should make it possible to reach even smaller dimensions allowed by the small wavelength (13.4 nm in this experiment). Even though e-beam written gratings are a prerequisite for this interference scheme to work, one can use the frequency multiplication in an iterative fashion to further increase the resolution, by multiplying the frequency by a factor of two in each step. For example, 120 nm period gratings written with e-beam can be used to make 60 and 30 nm period gratings in succession. Alternatively high-resolution gratings made with interference lithography in the ultraviolet range can be used as mother gratings to start this process. The technique should be useful in applications requiring extremely high-resolution periodic patterns that are not available from e-beam lithography techniques either due to resolution or throughput limitations.

Acknowledgements

The authors thank B. Haas and S. Stutz for help with preparation of the diffraction grating masks.

References

[1] A. Yen, M.L. Schattenburg, H.I. Smith, Appl. Optics 31 (1992) 2972.
[2] H.H. Solak, D. He, W. Li, S. Singh-Gasson, F. Cerrina, B.H. Sohn, X.M. Yang, P. Nealey, Appl. Phys. Lett. 75 (1999) 2328.
[3] M. Wei, D.T. Attwood, T.K. Gustafson, J. Vac. Sci. Technol. B 12 (1994) 3648.
[4] H.H. Solak, C. David, J. Gobrecht, L. Wang, F. Cerrina, Microelectron. Eng. 61 (2002) 77.
[5] H.H. Solak, W. Li, D. He, J. Wallace, F. Cerrina, AIP Conf. Proc. 521 (2000) 99.
[6] H.H. Solak, C. David, J. Gobrecht, L. Wang, F. Cerrina, J. Vac. Sci. Technol. B 20 (2002) 2844.
[7] A. Fernandez, D.W. Phillion, Appl. Optics 37 (1998) 473.